УДК 614.841.42:551.511.61 doi.org/10.31717/2311-8253.23.2.8

T. D. Lev, M. M. Talerko, B. S. Prister

Institute for Safety Problems of Nuclear Power Plants, NAS of Ukraine, 12, Lysohirska st., Kyiv, 03028, Ukraine

Comprehensive Assessment of the Chornobyl Exclusion Zone Wildfires Impact on the 100-km Area Around the Chornobyl NPP

Keywords:
Exclusion Zone,
mapping,
aerial pollution,
radioecological zoning,
geoinformational analysis,
radioecological criticality
of the territory

A comprehensive assessment of the impact of wildfires in the Chornobyl Exclusion Zone on the adjacent territory within a radius of 100 km in the spring of 2020 and 2022 was carried out, considering the potential and realized radioecological criticality of the territory. The realized radioecological criticality was expressed in the estimated specific activity of ^{137}Cs in plants, which was formed as a result of aerial and root pollution of agricultural vegetation in farm fields and gardens during the transfer and deposition of radionuclides during fires. The specific activity of ^{137}Cs in plants was calculated based on the data on the integrated volumetric activity of ^{137}Cs, obtained by the WRF-LEDI model of atmospheric transport, using the set of models "AeralPlant — SoilPlant" depending on the biological stage of plant development. According to the results of the calculations, thematic mapping was carried out with the selection of zones of maximum and minimum contamination of the territory, taking into account potential radioecological criticality. Regardless of the volume activity of ^{137}Cs in the air and the direction of air transfer, the spatial nature of the distribution of the most critical areas is preserved. As a result, the most critical areas were identified, where dangerous levels of radiation exposure on the population are possible due to atmospheric transport of radionuclides caused by wildfires and extreme weather phenomena (dust storms) in the Chornobyl Exclusion Zone. Different scenarios of the regional land use structure were considered and thematic assessment maps were built, which are the basis of preventive planning of rehabilitation measures in case of critical situations in accordance with radiation safety norms.

Introduction

As of today, we have obtained and analyzed the results of research on the quantitative assessment of the main factors determining the level of air pollution with radionuclides in the contaminated areas of the Exclusion Zone and areas of mandatory (obligatory) evacuation as well as radionuclides transfer to relatively clean territories under normal conditions and as a result of extreme weather events [1–5]. These factors include natural wind and anthropogenic resuspension of radioactive aerosols, as well as resuspension of radioactive aerosols into the atmosphere caused by wildfires and burning of grasslands in contaminated areas. Wildfires cause significant damage to the environment, quality of human life, the efficiency of human activities, and the overall economy of the country. Environmental and economic damage from wildfires in radioactively contaminated areas also includes losses resulting from the pollution of air and vegetation with combustion products containing radioactive elements.

A comprehensive assessment of the impact of the Chornobyl Exclusion Zone (ChEZ), contaminated as a result of the Chornobyl Nuclear Power Plant (ChNPP) accident in 1986, on the adjacent areas within a radius

of 100 km was conducted based on the results of wildfires and dust storms during the spring periods of 2020 and 2022 [6, 7]. These two periods differed in the causes of the fires:

the 2020 period (April) was associated with massive wildfires and extreme weather conditions (lack of moisture, strong winds, plough-disturbance of agricultural fields, etc.);

the 2022 period (March) was associated with the military actions of the Russian Federation against Ukraine within the ChEZ surrounding the nuclear power plant.

A comparative assessment of the two periods mentioned above was carried out based on the results of numerical modeling of the atmospheric transport and deposition of radioactive elements (^{137}Cs) onto the ground surface, along with calculations for the contamination of agricultural products and identification of critical areas. This assessment utilized the following models:

1) WRF-LEDI set of models forecasting aerometeorological conditions and atmospheric transport of radionuclides and their deposition on the underlying surface [8];

2) "AeralPlant — SoilPlant" set of models for ChNPP 100-km area plant products aerial and root contamination of plant products with radionuclides for ChNPP 100-km area [9].

2020 and 2022 wildfires natural conditions overview

April 3–22, 2020 wildfires period. From April 3rd to April 20th, the ChEZ experienced the largest wildfire in its history. Simultaneously, from April 16th to April 17th, 2020, Kyiv and Zhytomyr regions in north of Ukraine faced a strong dust storm which had an impact on the radiation environment within both the ChEZ and adjacent areas of the 100-kilometer zone around the ChNPP. The interaction of these two processes resulted in a synergetic intensification of the influx of radionuclides into the air. Specifically, strong winds in the lower atmosphere of the ChEZ on April 16th, 2020, contributed to the rekindling of wildfires on radioactively contaminated areas. By that moment, these fires had been nearly ceased by firefighting efforts and rain on April 14th. Burning of vegetation (especially in the meadow areas of the ChEZ), resulted in covering the ground surface in the period of April 3rd to April 13th with a layer of finely dispersed soil and ash particles, highly susceptible to intense wind resuspension [6].

Based on the analysis of surface synoptic charts, the dynamics of surface pressure and air temperature, as well as the directions of air mass movement, weather conditions during wildfires in the ChEZ in the period of April 4th to April 22nd, 2020, were categorized into six typical synoptic situations [10]. These situations were marked by the movement of southwesterly and westerly air masses (>30% of cases) at speeds not exceeding 2–3 m/s before April 15th. The average relative humidity of the air was around 50%, varying from 90% at night to 25% during the day. According to data from the meteorological station in Chornobyl, the last moderate-intensity precipitation (more than 3 mm per day) before the wildfires in the ChEZ occurred on March 10th, 2020. Starting from April 16th, after a cold front passage, wind speeds increased to 15–22 m/s at the surface and reached 30–40 m/s at higher altitudes. During this period, an extreme synoptic situation with intense short-term dust storm was observed.

March 16–29, 2022 wildfires period. Within this period wildfires in the ChEZ were associated with curtain weather conditions, which can be presented by two typical synoptic situations [10]: 1) from March 11th to March 23rd an anticyclonic situation prevailed, when weather conditions were influenced by an anticyclonic high-pressure pattern (baric field) with low velocity winds predominantly from the west, northwest, and north directions (80%) and clear and dry weather with a gradual seasonal increase in air temperature; 2) from March 24th to March 29th a cyclonic situation prevailed, resulting in rapid change of weather conditions due to the advection of cold air masses throughout the atmosphere, which entered Ukraine from the northwest, forming a cold front. Westerly and northwesterly (recurring 70% of the time) winds velocity at the lowest atmospheric layer reached 15–22 m/s. According to data from the Kyiv meteorological station, short-term showers with intensity up to 2 mm/12 hours were observed on March 24th and 26th.

Wildfires in the ChEZ mainly affected the areas used for agricultural production before the Chornobyl accident and largely covered with grassy vegetation now. This very conclusion — a relatively small area of forestlands was affected by fires — can be additionally illustrated by the vegetation map drafted in the post-Chornobyl period (Fig. 1).

It should be noted, that the fires in 2022 partially occurred in the same areas where they occurred in April 2020 (Fig. 2), mainly in the southwestern part of the ChEZ and in the vicinity of the villages Tovstyi Lis and Buda.

Radioactive aerosols atmospheric dispersion modelling and assessment of aerial contamination of vegetation

Calculations of the atmospheric dispersion of radioactive aerosols up to a distance of 100 km from the fire

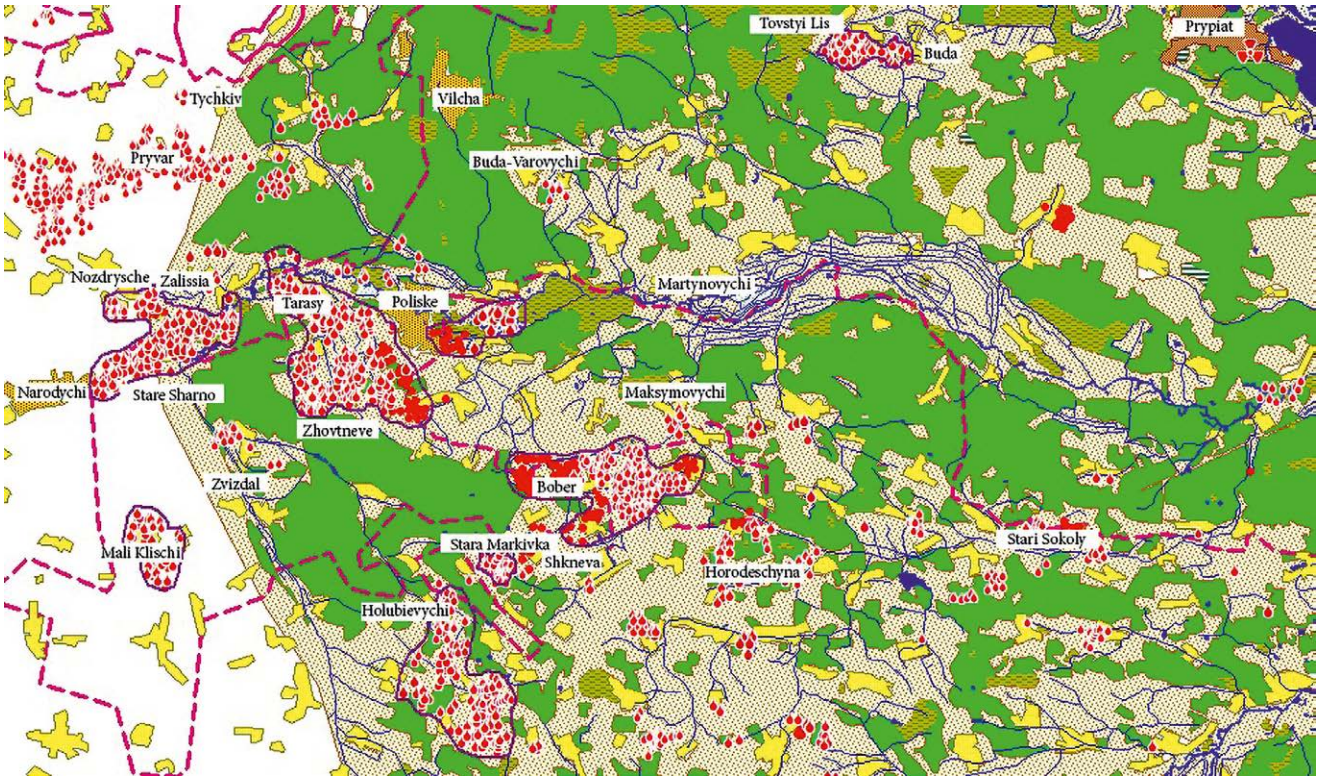

Fig. 1. 2022 fires areas on the vegetation map (see Figs 1–9 in color on the journal website)

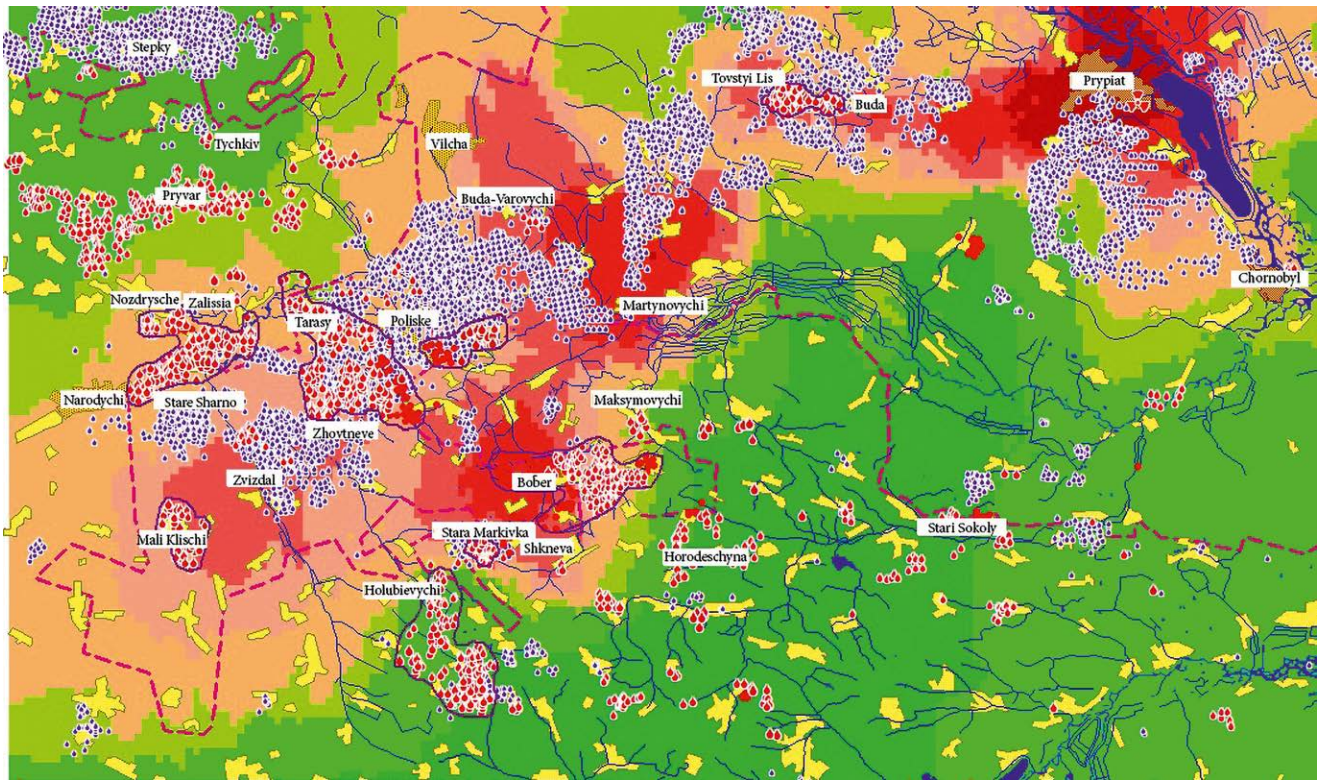

Fig. 2. 2020 fires areas (blue dots) and 2022 fires areas (red dots)

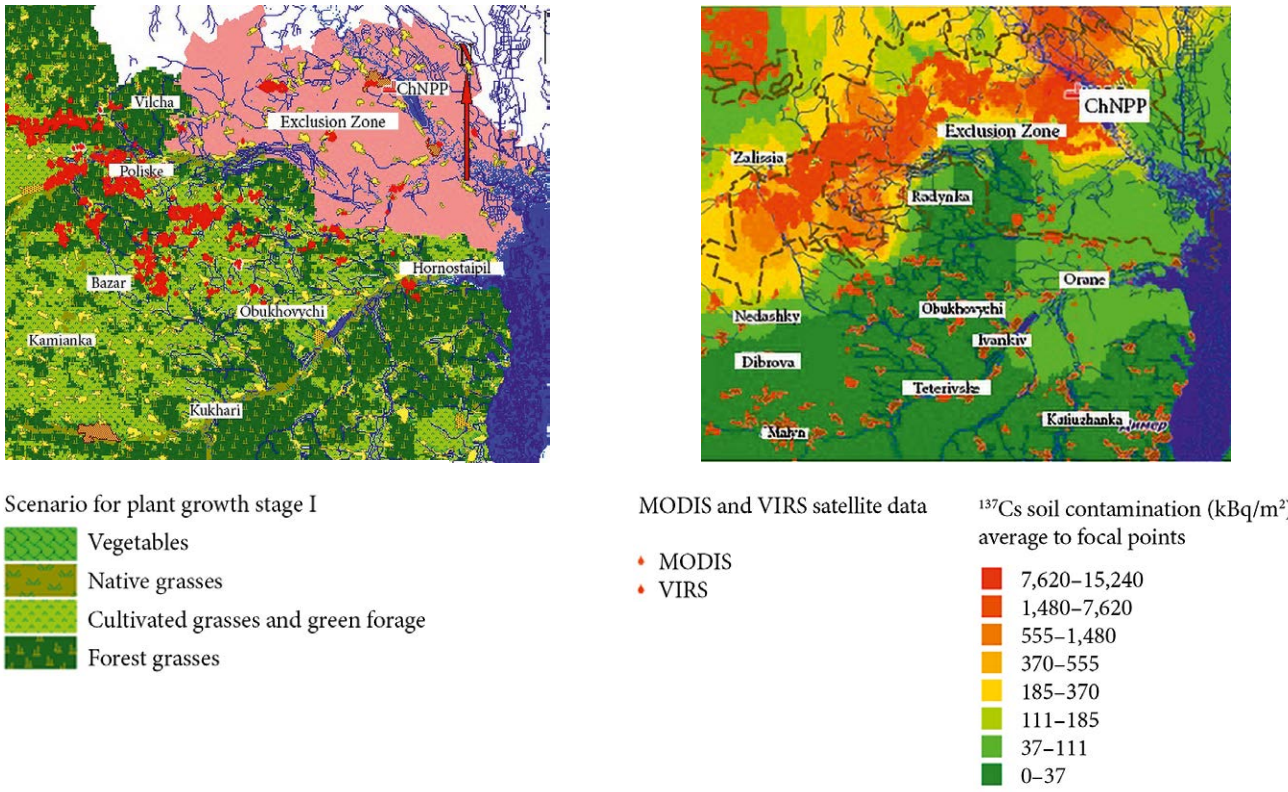

Fig. 3. April 16th and 17th, 2020 vegetation cover scenario — plant growth stage I (a), ChNPP 100-km zone ^{137}Cs soil contamination chart map (b)

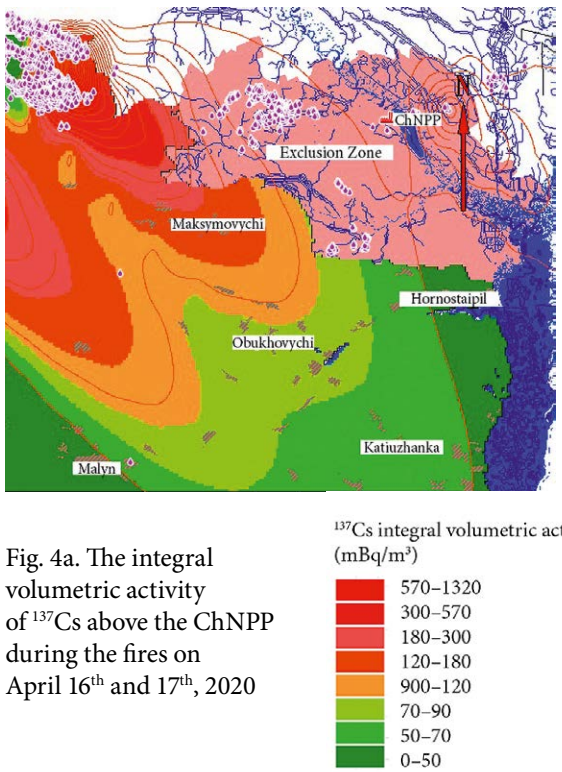

Fig. 4a. The integral volumetric activity of ^{137}Cs above the ChNPP during the fires on April 16th and 17th, 2020

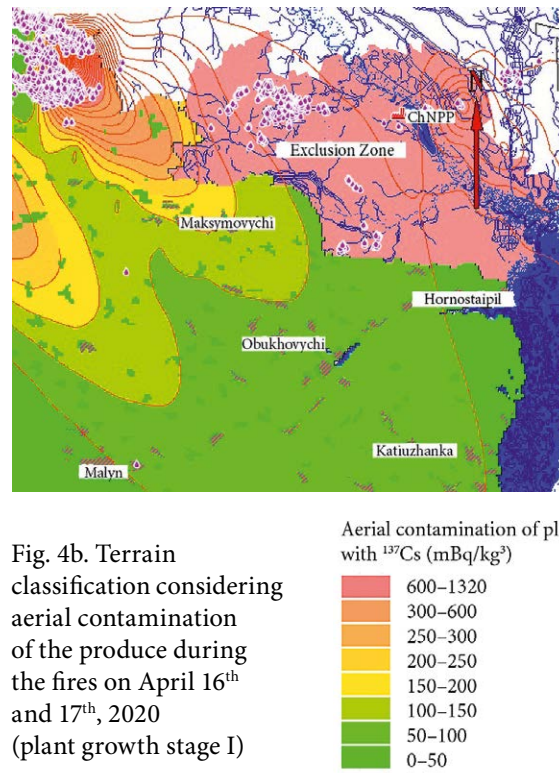

Fig. 4b. Terrain classification considering aerial contamination of the produce during the fires on April 16th and 17th, 2020 (plant growth stage I)

Table 1. Scenarios for assessment of aerial contamination of specific plant species

Case scenario No.	Scenario code	Plant species	Validity period	*KP* ^{137}Cs
1	Scen_1kv*	Herbage	1st qtr. 10.04–20.05	200
		Grain crops, stage I		0.35
		Forest grasses		200
		Garden greens		200
2	Scen_2kv	Grass, greens	2nd qtr. 20.05–30.06	200
		Grain crops, stage I		0.35
		Potatoes, stage I		3
		Cabbage and root crops, stage I		0.7
		Cucumbers and tomatoes, stage I		0.3
3	Scen_3kv	Grass, greens	3rd qtr. 30.06–01.08	200
		Grain crops, stage II		37
		Potatoes, stage II		0.06
		Cabbage and root crops, stage II		4.2
		Cucumbers and tomatoes, stage II		6.8
4	Scen_4kv	Grass, greens	4th qtr. 01.08–30.10	200
		Grain crops, stage I		0.35
		Potatoes, stage II		0.06
		Cabbage and root crops, stage II		4.2
		Cucumbers and tomatoes, stage II		6.8

* 1st quarter scenario (10.04–20.05): *KP* represents the transfer factor between the concentration of a specific radionuclide in plants and the density of deposition of that radionuclide on the ground, (Bq · kg^{-1}/kBq · m^{-2}) [11]

zone were carried out, providing an assessment of the integral (in time) volumetric concentration of ^{137}Cs in the surface air. To assess the aerial contamination of vegetation, a case scenario for 100-km zone land-use pattern was drafted, considering the vegetation growth stage and the levels of soil contamination with ^{137}Cs after the Chornobyl accident in 1986. Fig. 3a shows a map chart of the first scenario (Table 1) corresponding to the season (spring 2020) and the spatial distribution of ^{137}Cs soil contamination after the ChNPP accident (see Fig. 3b).

The concentration of radionuclides in plant biomass at time t after single deposition is calculated according to the formula [9]

$$C(t) = \mathrm{Dep}_{\mathrm{Cs}} \cdot KP \cdot (a_1 \cdot e^{-0{,}693 \cdot \frac{t}{T_1}} + (1 - a_1) \cdot e^{-0{,}693 \cdot \frac{t}{T_2}}), \quad (1)$$

where $C(t)$ is the concentration of the radionuclide in plants at time t after deposition (Bq · kg^{-1}); $\mathrm{Dep}_{\mathrm{Cs}}$ is the density of deposition of that radionuclide (kBq · m^{-2}); *KP* is transter factor (see Table 1); T_1 and T_2 are the half-life periods of the fast removable and slowly removable forms of the radionuclide, respectively; a_1 is the fraction of the fast removable form [11].

The density of ^{137}Cs deposition (mBq/m^2) on the leaf surface is calculated using the formula

$$\mathrm{Dep}_{\mathrm{Cs}} = A_{kt} \cdot V_d, \quad (2)$$

where A_{kt} is the daily integrated activity of ^{137}Cs in the air over the ChNPP 100-kilometer zone (mBq · s/m^3); V_d is the dry deposition velocity to the surface, given as $5 \cdot 10^{-3}$ m/s.

Using the WRF-LEDI atmospheric transport model set and the provided formulas (1) and (2), calculations were performed for the integral volumetric activity of ^{137}Cs in the air (Fig. 4a) and the specific activity of ^{137}Cs contamination of leafy vegetables and native grasses due to wildfires and dust storms on April 16th and 17th, 2020 (Fig. 4b). For this purpose, scenario maps for the agricultural crops zonation during the acute phase of the accident were used, along with the given transfer factors (KP) between the density of deposition and the specific activity of the radionuclide in the produce.

According to the modeling results (see Fig. 4b), following the period of fires with a dust storm on April 16th and 17th, 2020, the concentration of ^{137}Cs in leafy vegetables and grass within the selected region reached

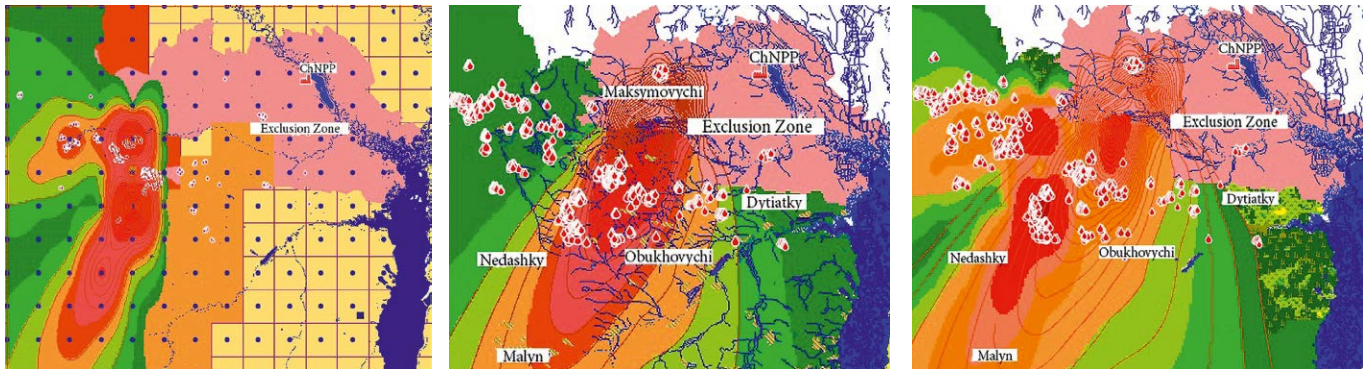

Integral volumetric activity of ^{137}Cs in the air (mBq/m^3) on March 11–18, 2022

- 80,000–136,000
- 40,000–80,000
- 20,000–40,000
- 15,000–20,000
- 10,000–15,000
- 5,000–10,000
- 1,000–5,000
- 1–1,000

Integral volumetric activity of ^{137}Cs in the air (mBq/m^3) on March 19–24, 2022

- 30,000–55,000
- 15,000–30,000
- 10,000–15,000
- 8,000–10,000
- 4,000–8,000
- 2,000–4,000
- 500–2,000
- 1–500

Integral volumetric activity of ^{137}Cs in the air (mBq/m^3) on March 11–24, 2022

- 100,000–150,000
- 50,000–100,000
- 36,000–50,000
- 24,000–36,000
- 12,000–24,000
- 9,000–12,000
- 6,000–9,000
- 3,000–6,000
- 1,000–3,000
- 1–1,000

a b c

Fig. 5. The spatial distribution of volumetric concentration of ^{137}Cs in the air according to the periods: March 11–18, 2022 to the north (a), March 19–24, 2022 to the northeast (b) and gross volumetric concentration of ^{137}Cs in the air on March 11–24, 2022 (c) after wildfires in ChEZ

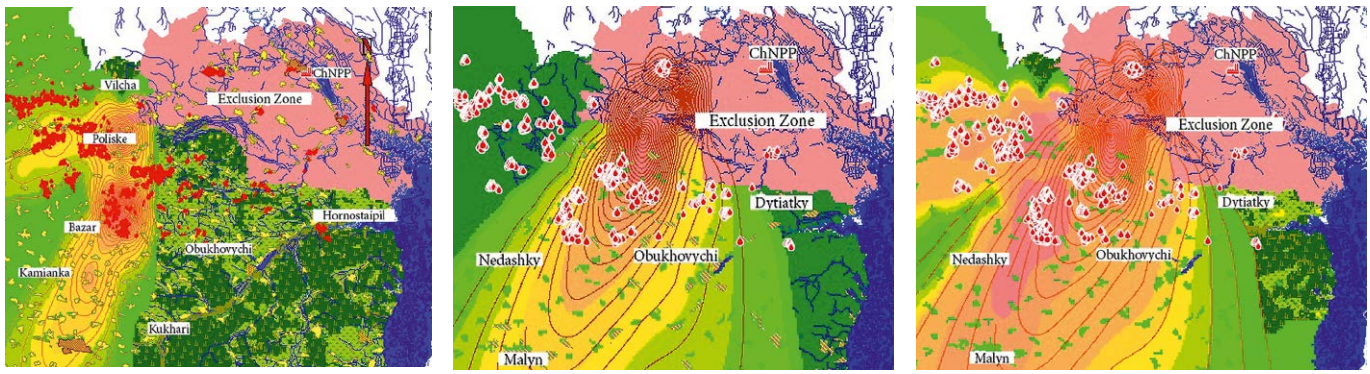

Produce aerial contamination on March 11–18, 2022 (mBq/kg)

- 70–135
- 54–70
- 36–54
- 18–36
- 12–18
- 6–12
- 3–6
- 0–3

Produce aerial contamination with ^{137}Cs on March 19–24, 2022 (mBq/kg)

- 30.3–54.8
- 17.7–30.3
- 11.3–17.7
- 7.6–11.3
- 4.8–7.6
- 2.5–4.8
- 0.7–2.5
- 0–0.7

Produce aerial contamination on March 11–24, 2022 (mBq/kg)

- 70–135
- 54–70
- 36–54
- 18–36
- 12–18
- 6–12
- 3–6
- 0–3

a b c

Fig. 6. The spatial distribution of plant produce contamination with ^{137}Cs according to the periods: March 11–18, 2022 (a), March 19–24, 2022 (b) and gross specific activity of ^{137}Cs in the produce on March 11–24, 2022 (c) after wildfires in ChEZ

a maximum value of 1,320 mBq · kg^{-1}, which is three orders lower than the operational intervention level OIL6 (IAEA criteria [12]) for a radiological accident, which is set at 2 kBq · kg^{-1}. Therefore, based on the calculations and comparison with intervention criteria, the results obtained after the fires and dust storm have practically no impact on the radiation exposure of the population residing in these areas.

Similarly, the consequences of fires during military operations in the ChEZ for the period from March 11th to March 24th, 2022 [7] had been assessed using the model set. The calculation period was divided into two periods, taking into account the direction of atmospheric transport: to the north (March 11–18, 2022) and to the northeast (March 19–24, 2022). The results of the spatial distribution of volumetric concentration, calculated using the WRF-LEDI model set, are presented on Fig. 5. Since the volumetric concentration values are small, they are given in μBq/m^3 and are an order of magnitude lower than the calculated values for the period of fires and dust storm on April 16th and 17th, 2020.

Using formula (1) and Table 1, the aerial contamination of produce resulting from wildfires and the transport of radionuclides to adjacent areas was calculated for two periods (Fig. 6 a and b), as well as the gross aerial contamination of produce for the entire period (c). The results show that the highest contamination of plant produce occurred during the period with northward atmospheric transport (March 11–18, 2022) from the areas of more intense wildfires.

The overall contamination of plant produce after the fires in the spring of 2022 was found to be an order of magnitude lower than the contamination after fires and dust storm in 2020.

Analysis of the results obtained

The realized radioecological criticality [13] was expressed in the calculated specific activity of ^{137}Cs in plants accumulated due to the aerial contamination of agricultural vegetation on farmland and gardens due to the transport and deposition of radionuclides during the fires in 2020 and 2022. The integral deposition for the specified period was taken into account along with empirically obtained transfer factors between the volumetric activity in the air and the specific activity in plants depending on the biological growth stage of the vegetation. Based on the calculation results, thematic mapping was carried out to identify zones of maximum and minimum contamination of the territory, as well considering potential radioecological criticality [13, 14]. The consideration of radioecological criticality was conducted as follows:

on the comprehensive map (Fig. 7) of potential radioecological criticality using GIS tools, three spatial zones with an elevated degree of criticality were identified, corresponding to the specified map (the range of values for the potential criticality parameter is 0.502–0.648);

these zones were delineated as separate regions that can be overlaid onto any thematic map (for aerial or root contamination of vegetation) to determine the most critical areas for further analysis and decision-making.

The chart map below (Fig. 8) represents the ChNPP 100-km area (without ChEZ) zoning based on classes with the highest degree of criticality [14]:

class 114 — agricultural lands located on superaquatic landscapes with peat soils in river floodplains with herbaceous vegetation (cereal crops in vegetative growth stage II) cover an area of 77.22 km^2;

class 124 — agricultural lands located on eluvial landscapes with soddy gleyed light loamy soils and herbaceous vegetation (cereal crops in vegetative growth stage II) cover an area of 44.66 km^2;

class 134 — agricultural lands located on downslope landscapes with soddy gleyed light loamy soils and herba-

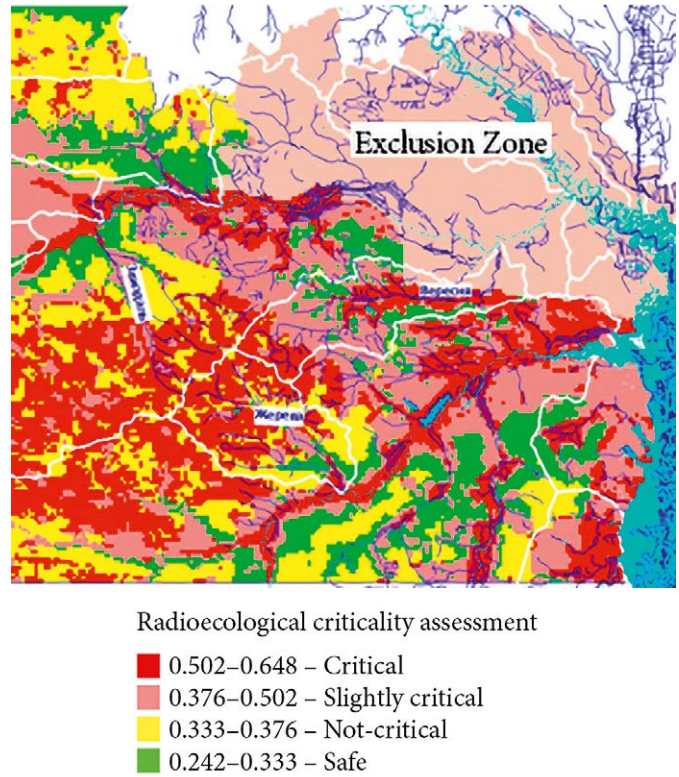

Fig. 7. Comprehensive map of potential radioecological criticality of the ChNPP 100-km zone according to typological zones

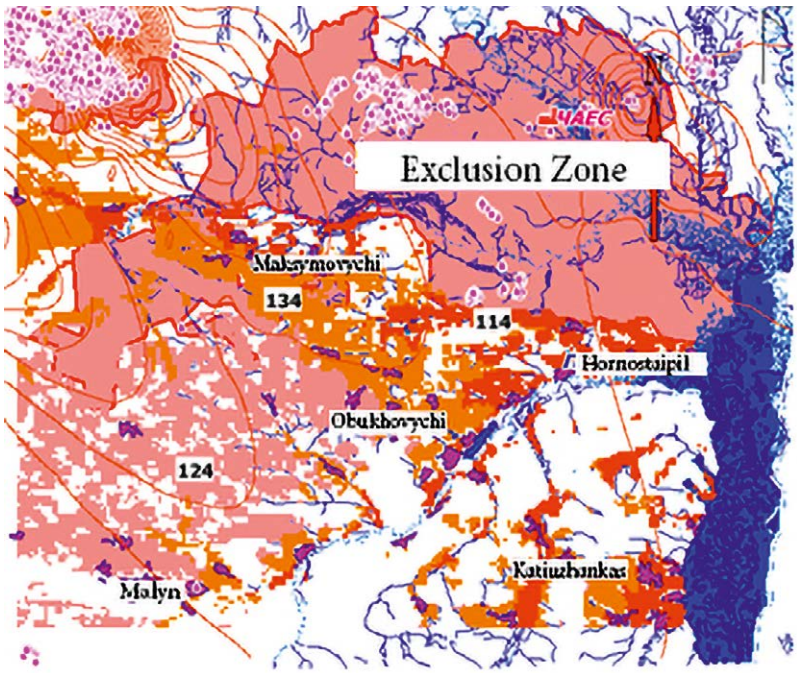

Fig. 8. ChNPP 100-km area criticality zoning

ceous vegetation (cereal crops in vegetative growth stage II) cover an area of 110.91 km^2.

Classes of criticality are also distinguished within the territory of populated areas with gardens and meadow vegetation. In our example, for the analyzed territory of the ChNPP 100-km zone, these types of underlying terrain are not representative, except for the forested areas, which are not critical.

For the highlighted classes of criticality, average values, maximum, and minimum values of the specific activity of ^{137}Cs in plants were obtained for the period of fires and dust storms on April 16th and 17th, 2020 (Table 2).

The comparative data provided on the Fig. 9 suggest that areas with elevated levels of product contamination do not necessarily coincide with the designated criticality classes. However, the map highlights regions with maximum product contamination (calculated using the model) within different criticality classes. This presentation allows for the prioritization of areas for further environmental protection measures in the event of particularly hazardous extreme situations in radioactive contamination areas.

Table 2. Statistical data on calculated specific activity of ^{137}Cs in plants according to radioecological criticality classes, mBq/kg

Criticality class	Average value	Minimal value	Maximal value
114	82.3	0.7	343.2
124	100.7	1.16	1 044.1
134	125.5	27.8	1 117.2

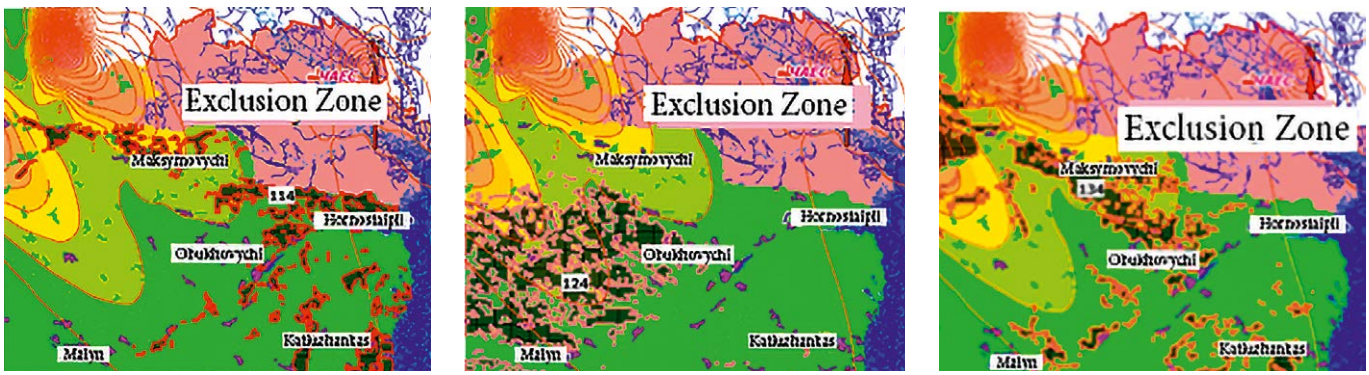

Fig. 9. Spatial distribution of radioecological classes (114, 124, 134) on the thematic map of gross specific activity of ^{137}Cs in plants within the period of fires and dust storm on April 16th and 27th, 2020

Conclusions

A set of mathematical models has been developed for assessing and forecasting radioactive contamination of the atmosphere, redistribution of radionuclides within the components of the environment due to extreme meteorological events (wildfires, tornadoes, dust storms), and man-made impact within the ChEZ and beyond.

As a result, the most critical areas with the potential for dangerous levels of radiation exposure to the population due to atmospheric transport of radionuclides from the ChEZ in case of wildfires and extreme meteorological events (dust storms) have been identified. The findings show that the most significant contamination of agricultural produce occurred during the period with northward atmospheric transport (March 11–18, 2022) from the areas of relatively larger sources of wildfires. Various scenarios of regional land use patterns have been considered, and thematic assessment maps have been drafted as a base for preventive planning of rehabilitation measures in critical situations according to radiation safety standards.

References

1. Prister B. S., Kluchnikov A. A., Bariakhtar V. G., Shestopalov V. M., Kukhar V. P. (2016). *Problemy bezopasnosti atomnoy energetiki. Uroki Chernobylya* [Nuclear power Security Issues. Chornobyl lessons]. Chornobyl, 356 p. (in Rus.)
2. Goldammer J. G., Kashparov V., Zibtsev S., Robinson S. (2015). *Peredovoy opyt bor'by s prirodnymi pozharami na zagryaznennykh territoriyakh i rekomendatsii po bezopasnosti pozharnykh pri pozharakh na territoriyakh s radioaktivnym zagryazneniyem* [Best practices and recommendations for wildfire suppression in contaminated areas, with focus on radioactive terrain]. Global Fire Monitoring Center (GFMC)]. Freiburg — Basel — Kyiv. 45 p. (in Rus.)
3. Evangeliou N., Zibtsev S., Myroniuk V., Zhurba M., Hamburger T., Stohl A., Balkanski Y., Paugam R., Mousseau T. A., Møller A. P., Kireev S. I. (2016). Resuspension and atmospheric transport of radionuclides due to wildfires near the Chernobyl Nuclear Power Plant in 2015: An impact assessment. *Scientific Reports*, vol. 6, art. 26062.
4. Talerko M. M., Lev T. D., Kireev S. I., Kashpur V. O., Kuzmenko G. G. Evaluation of radioactive air contamination due to a forest fire within the Exclusion Zone on June 5–8, 2018. *Nuclear Power and the Environment*, vol. 2 (14), pp. 47–57.
5. Press release of the Regional Eastern European Fire Monitoring Center regarding fires near the Chornobyl Exclusion Zone on March 29, 2020 — April 16, 2020. Available at: https://nubip.edu.ua/node/75436. (in Ukr.)
6. Talerko M. M., Lev T. D., Kovalets I. V., Yatsenko Yu. V. (2020). [Modeling of the atmospheric distribution of radioactivity released into the air as a result of wildfires in the Exclusion Zone in April 2020]. *Nuclear Power and the Environment*, vol. 3 (18), pp. 86–104. (in Ukr.)
7. Talerko M., Lev T., Nosovskyi A. (2022). [Assessment of radioactive contamination of the atmosphere due to wildfires in the exclusion zone in the period from March 11 to March 31, 2022]. Proceedings of the *INUDECO 2022 International Conference "Problems of Decommissioning of Nuclear Energy Facilities and Environmental Restoration" (Slavutych, April 27–28, 2022).* (in Ukr.)
8. Talerko N. N., Garger E. K., Klyuchnikov A. A. (2010). Prediction of the consequences of accidental releases from nuclear power plants with the help of the mesoscale atmospheric transport model LEDI. *Reports of the National Academy of Sciences of Ukraine*, vol. 12, pp. 74–79. (in Rus.)
9. Prister B. (2022). Model of radionuclide uptake by plants via foliar pathway: Kyshtym, Chernobyl, Fukushima. In: Nanba K., Konoplev A., Wada T. (eds.) *Behavior of Radionuclides in the Environment III*. Singapore: Springer, 389–424. doi.org/10.1007/978–981–16–6799–2_18.
10. Lev T. D., Talerko M. M. (2022). [Analysis and modeling of meteorological conditions of radionuclide distribution during wildfires and dust storms in the Chornobyl Exclusion Zone in 2015–2022 using reanalysis data]. *Nuclear Power and the Environment,* vol. 2 (24), pp. 67–85. (in Ukr.)
11. Prister B. S. (2008). *Problemy sel'skokhozyaystvennoy radioekologii i radiobiologii pri zagryaznenii okruzhayushchey sredy molodoy smes'yu produktov yadernogo deleniya* [Problems of agricultural radioecology and radiobiology in the influence of the environment with a young mixture of nuclear fission products]. Chornobyl: ISP NPP, NAS of Ukraine, 320 p. (in Rus.)
12. IAEA (2012). *Criteria for use in preparedness and response to a nuclear or radiological emergency*. IAEA Safety Standards, No. GSG-2. Vienna: International Atomic Energy Agency, 132 p. (in Rus.)
13. Prister B. S., Vinogradskaya V. D., Lev T. D, Talerko M. M., Garger E. K., Onishi Y., Tischenko O. G. (2018). Preventive radioecological assessment of territory for optimization of monitoring and countermeasures after radiation accidents. *Journal of Environmental Radioactivity*, vol. 184–185, pp. 140–151. doi.org/10.1016/j.jenvrad.2018.01.021.
14. Prister B. S., Lev T. D., Nosovskyi A. V., Talerko M. M. (2022). *Comprehensive radioecological monitoring for objects of radioactively contaminated areas*. Kyiv: Akademperiodyka, 286 p.

Т. Д. Лев, М. М. Талерко, Б. С. Прістер

Інститут проблем безпеки АЕС НАН України, вул. Лисогірська, 12, Київ, 03028, Україна

Комплексна оцінка впливу лісових пожеж у зоні відчуження на територію 100-км зони навколо Чорнобильської АЕС

Виконано комплексну оцінку впливу лісових пожеж у Чорнобильській зоні відчуження на прилеглу територію в радіусі 100 км навесні 2020 та 2022 рр. з урахуванням потенційної та реалізованої радіоекологічної критичності території. Реалізована радіоекологічна критичність виражалася в розрахунковій питомій активності ^{137}Cs у рослинах, що сформувалась унаслідок аерального та кореневого забруднення сільськогосподарської рослинності на фермерських полях та городах при перенесенні та осадженні радіонуклідів у період пожеж. Питома активність ^{137}Cs у рослинах розраховувалася за даними про інтегральну об'ємну активність ^{137}Cs, отриманими за моделлю атмосферного перенесення WRF-LEDI, з використанням комплексу моделей "AeralPlant — SoilPlant" залежно від біологічної фази розвитку рослин. За результатами розрахунків було проведено тематичне картографування з виділенням зон максимального та мінімального забруднення території з урахуванням потенційної радіоекологічної критичності. Незалежно від величини об'ємної активності ^{137}Cs у повітрі та напрямку повітряного перенесення просторовий характер розподілу найбільш критичних територій зберігається. У результаті було виявлено найбільш критичні території, на яких можливе формування небезпечних рівнів дозового навантаження на населення при повітряному перенесенні радіонуклідів із зони відчуження внаслідок лісових пожеж та екстремальних метеорологічних явищ (пилові бурі) у Чорнобильській зоні відчуження. Розглянуто різні сценарії структури регіонального землекористування та побудовано тематичні оціночні карти, які є основою превентивного планування реабілітаційних заходів у випадку критичних ситуацій відповідно до норм радіаційної безпеки.

Ключові слова: зона відчуження, картографування, аеральне забруднення, радіоекологічне районування, геоінформаційний аналіз, радіоекологічна критичність території.

Надійшла 09.06.2023
Received 09.06.2023